Electronic Supplementary Material (ESI) for Environmental Science: Nano.

Supporting Information

Criteria of active sites in nonradical persulfate activation process from integrated experimental and theoretical investigations: boron-nitrogen-co-doped nanocarbons mediated peroxydisulfate activation as an example

Chunyang Nie [a#], Zhenhua Dai [a#], Wenjie Liu [a], Xiaoguang Duan [b], Chengyin Wang [c], Bo Lai [d], Zhimin Ao [a]*, Shaobin Wang [b], Taicheng An [a]

[a] *Guangdong Key Laboratory of Environmental Catalysis and Health Risk Control, Guangzhou Key Laboratory of Environmental Catalysis and Pollution Control, School of Environmental Science and Engineering, Institute of Environmental Health and Pollution Control, Guangdong University of Technology, Guangzhou 51006, China;*

[b] *School of Chemical Engineering and Advanced Materials, the University of Adelaide, Adelaide, SA 5005, Australia*

[c] *College of Chemistry and Chemical Engineering, Jiangsu Key Laboratory of Environmental Engineering and Monitoring, Yangzhou University, Yangzhou, 225002, China;*

[d] *State Key Laboratory of Hydraulics and Mountain River Engineering, College of Architecture and Environment, Sichuan University, Chengdu 610065, China*

* Corresponding authors: *E-mail:* zhimin.ao@gdut.edu.cn (ZA)

Pages - 15
Texts - 2
Tables - 2
Figures - 14

Text S1 To condute Density Functional Theory calculations, the electron exchange-correlation interactions were treated by the Perdew-Burke-Ernzerhof exchange correlation function in the scheme of generalized gradient approximation.[1] Double numerical plus polarization was employed as the basis set. The convergence tolerance of energy of 10^{-5} Hartree was applied (1 Hartree = 27.21 eV), and the maximal allowed force and displacement were 0.002 Hartree/Å and 0.005 Å, respectively. A global orbitals cut off of 4.1 Å was used and the van der Waals forces, which has been proved to be very important for adsorption calculation,[2,3] was taken into consideration by DFT+D method within the TS scheme[4] in all the calculations. The 18×18 Å^2 graphene matrix with non-periodic boundary conditions terminated by H atoms as the initial model was applied in the simulations and all the atoms were allowed to fully relax.

Text S2 Calculation of pseudo-second-order reaction rate constant and pseudo-first-order reaction rate constant is based on the following equations:

pseudo-second-order reaction: $\frac{1}{C_t} = k_2 t + \frac{1}{C_0}$

pseudo-first-order reaction: $\ln(\frac{C_0}{C_t}) = k_1 t$

where k_1 represents the pseudo-first-order reaction rate constant (min^{-1}), k_2 represents the pseudo-second-order reaction rate constant (mM^{-1}min^{-1}), C_0 is the initial phenol concentration, C_t is the phenol concentration at time t during the oxidation by activated PDS.

Tables

Table S1. The kinetics of phenol oxidation in BCN-NT/NS composites/PDS and N-rGO/PDS systems.

Samples	pseudo-second-order reaction		pseudo-first-order reaction	
	Rate constant ($mM^{-1}min^{-1}$)	R^2	Rate constant (min^{-1})	R^2
N-rGO	0.0079±0.0002	0.845	0.0085±0.0002	0.915
BCN-NT/NS-1	0.0125±0.0004	0.927	0.0111±0.0001	0.911
BCN-NT/NS-6	0.0167±0.0001	0.986	0.0141±0.0002	0.951
BCN-NT/NS-8	0.0278±0.0006	0.991	0.0187±0.0002	0.968
BCN-NT/NS-10	0.0172±0.0008	0.997	0.0140±0.0003	0.96
BCN-NT/NS-8_800	0.0095±0.001	0.953	0.0097±0.0007	0.935
BCN-NT/NS-8_1000	0.005±0.0005	0.966	0.0067± 0.0003	0.963

Table S2. The calculated adsorption energy (E_{ads}), the quantity of atomic charge on $S_2O_8^{2-}$ anion by Hirshfeld analysis (Q), O-O bond length (l_{O-O}) of SO_4-SO_4 and S-O bond length (l_{S-O}), and electrophilic index (ω) of $S_2O_8^{2-}$ adsorbed on pristine graphene and different doped graphene structures.

	Functionality	E_{ads}(eV)	Q(e)	l_{O-O}(Å)	l_{S-O}(Å)	ω
Graphene	sp^2 C	-2.37	-1.06	1.40	1.85	0.20
N-doped graphene	gN*i*	-2.78	-1.15	1.41	1.82	0.34
	gN*z*	-3.13	-1.18	1.38	1.99	0.19
	pdN*z*	-2.44	-0.95	1.31	2.04	0.19
	gN*a*	-2.89	-1.02	1.33	2.01	0.22
	pdN*a*	-2.12	-1.21	1.42	1.82	0.21
	prN	-2.85	-1.03	1.40	1.85	0.09
B-doped graphene	B*z*	-2.10	-0.95	1.37	1.90	0.23
	B*i*	-2.00	-0.92	1.36	1.93	0.02
	B*a*	-1.92	-0.92	1.36	1.92	0.05
	BC_2O	-2.86	-0.82	1.47	1.79	0.30
	BCO_2	-2.93	0.92	1.48	1.78	0.22
B, N-co-doped graphene	B*a*-C-gN*a*	-1.77	-0.86	1.33	2.00	0.09
	B*i*-C-N	-2.43	-1.03	1.37	1.90	0.19
	B-pdN*z*	-2.50	-0.94	1.49	1.82	0.22
	B*z*-C-prN	-2.65	-0.91	1.48	1.76	0.29
	BCO_2-gN*z*	-3.70	-0.96	1.49	1.78	0.31
	B-gN*a*	-2.38	-0.94	1.33	2.01	0.46
	B*z*-C-gN*z*	-3.01	-0.82	1.49	1.68	0.65

Figures

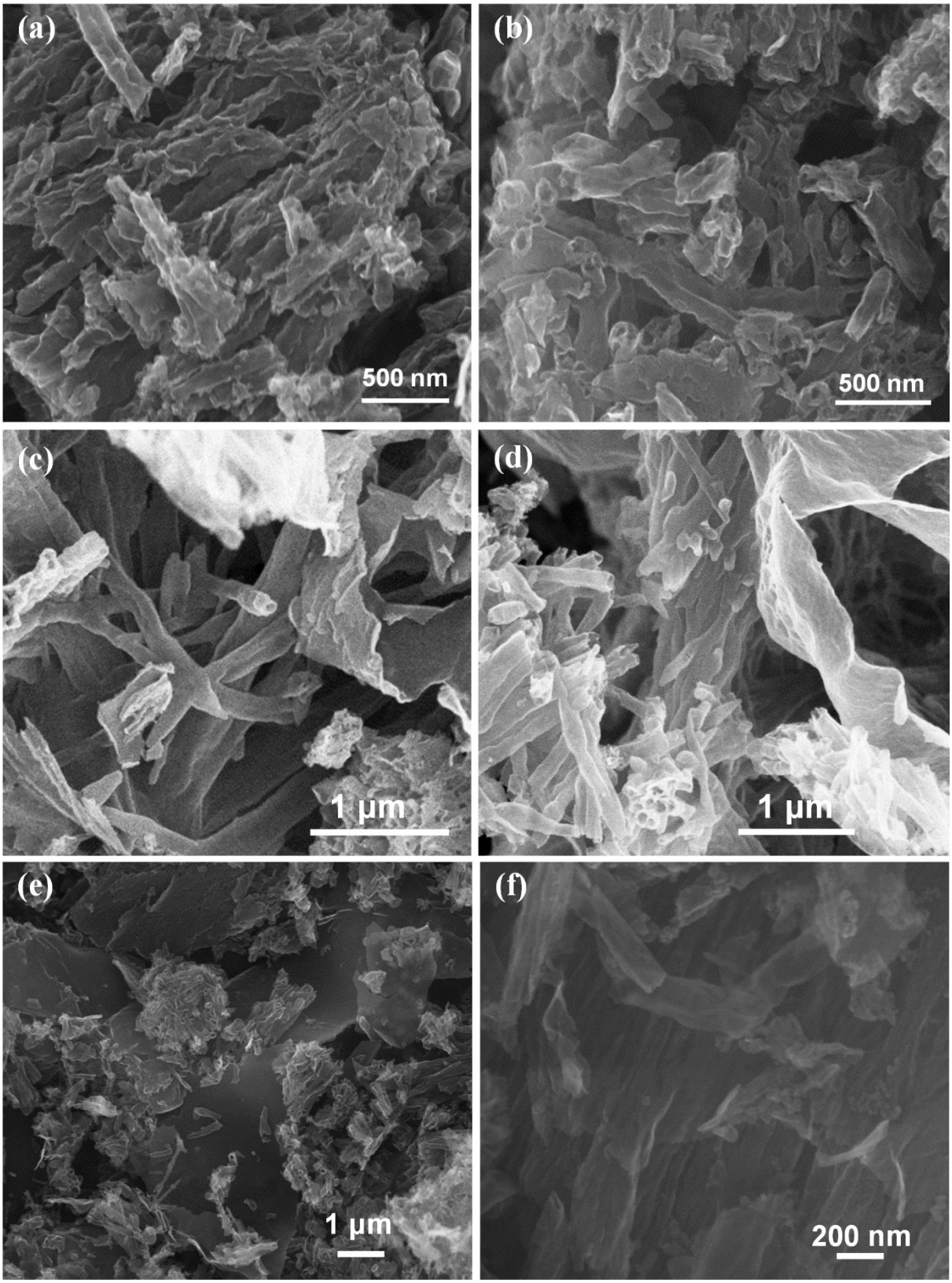

Figure S1. SEM images of (a) BCN-NT/NS-1; (b) BCN-NT/NS-6; (c) BCN-NT/NS-8; (d) BCN-NT/NS-10; (e) BCN-NT/NS-8_800 and (d) BCN-NT/NS-8_1000.

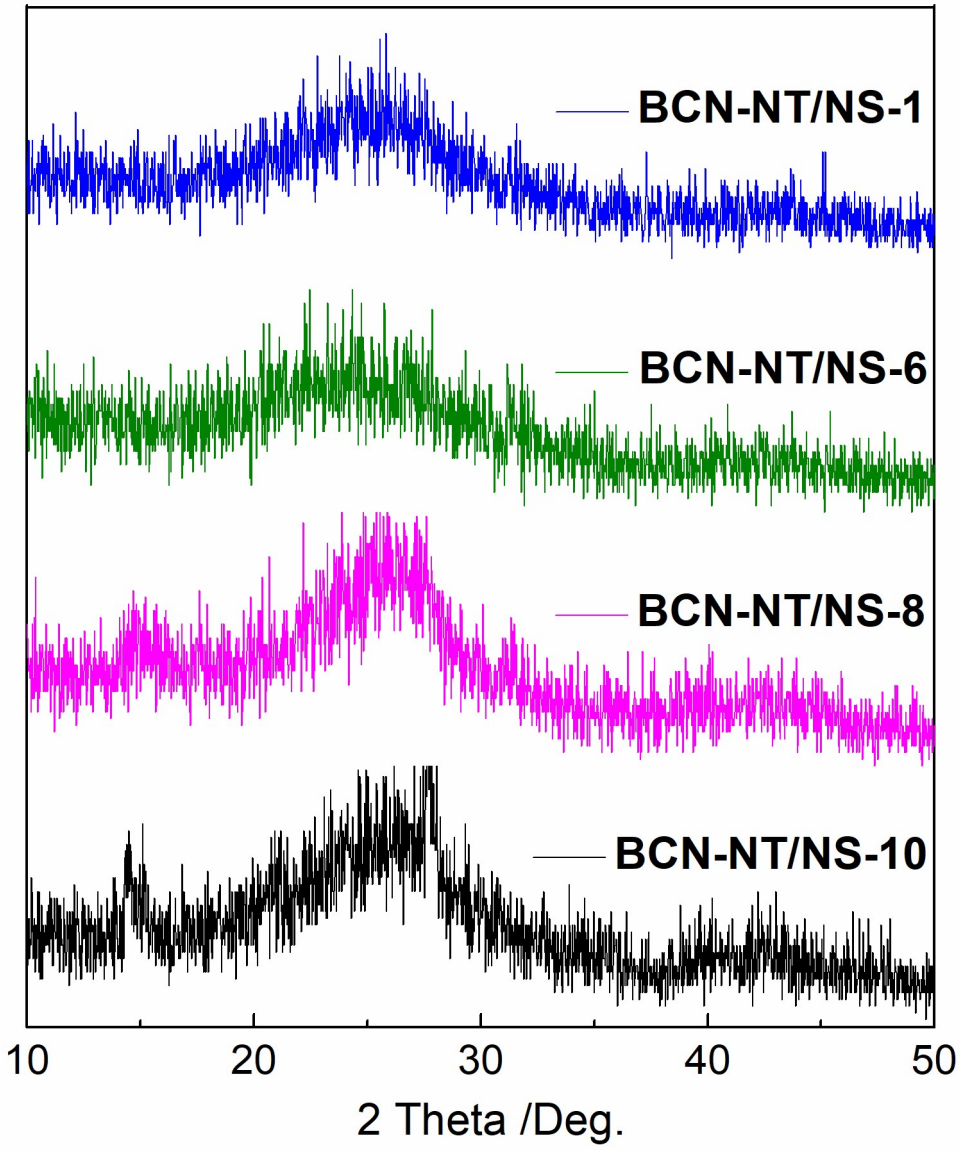

Figure S2. XRD spectra of the as-prepared BCN-NT/NS composites.

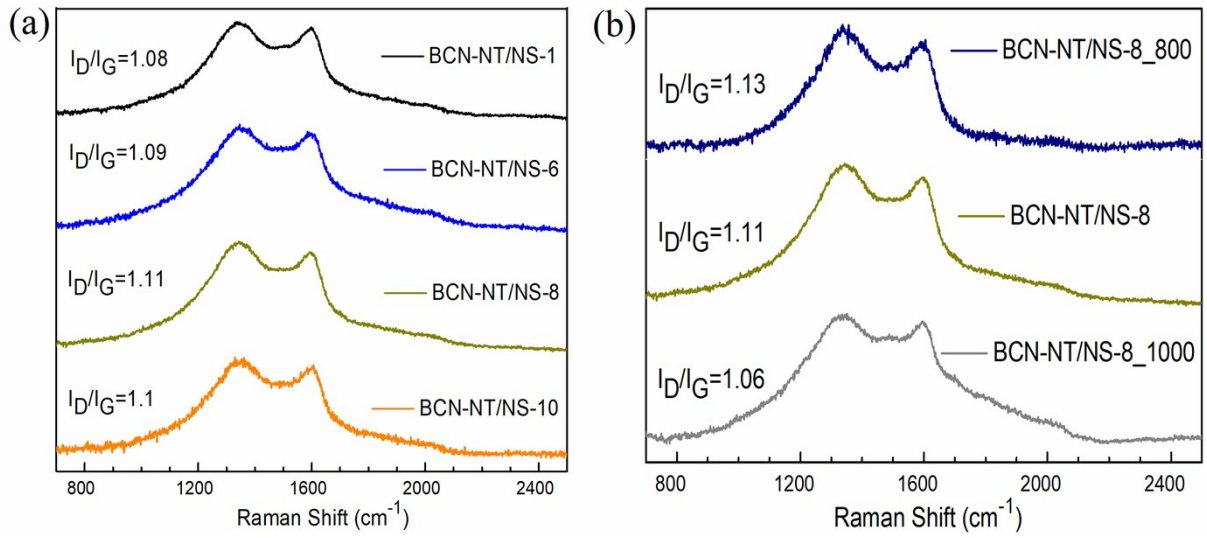

Figure S3. Raman spectra of (a) BCN-NT/NS composites prepared with different PEG precursors; (b) BCN-NT/NS composites prepared at different temperatures.

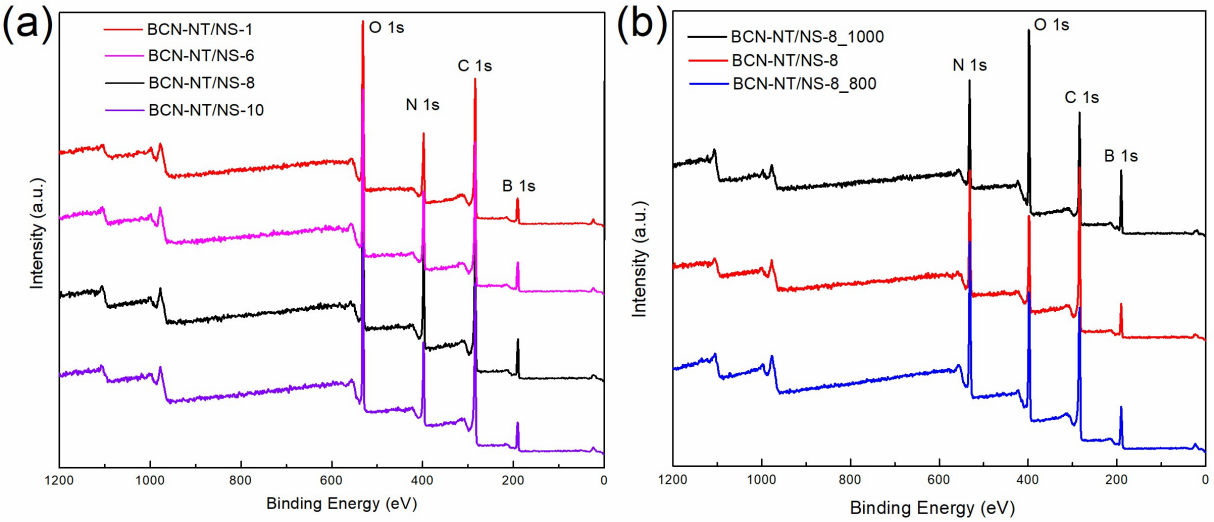

Figure S4. XPS survey spectra of (a) BCN-NT/NS composites prepared with different PEG precursors; (b) BCN-NT/NS composites prepared at different temperatures.

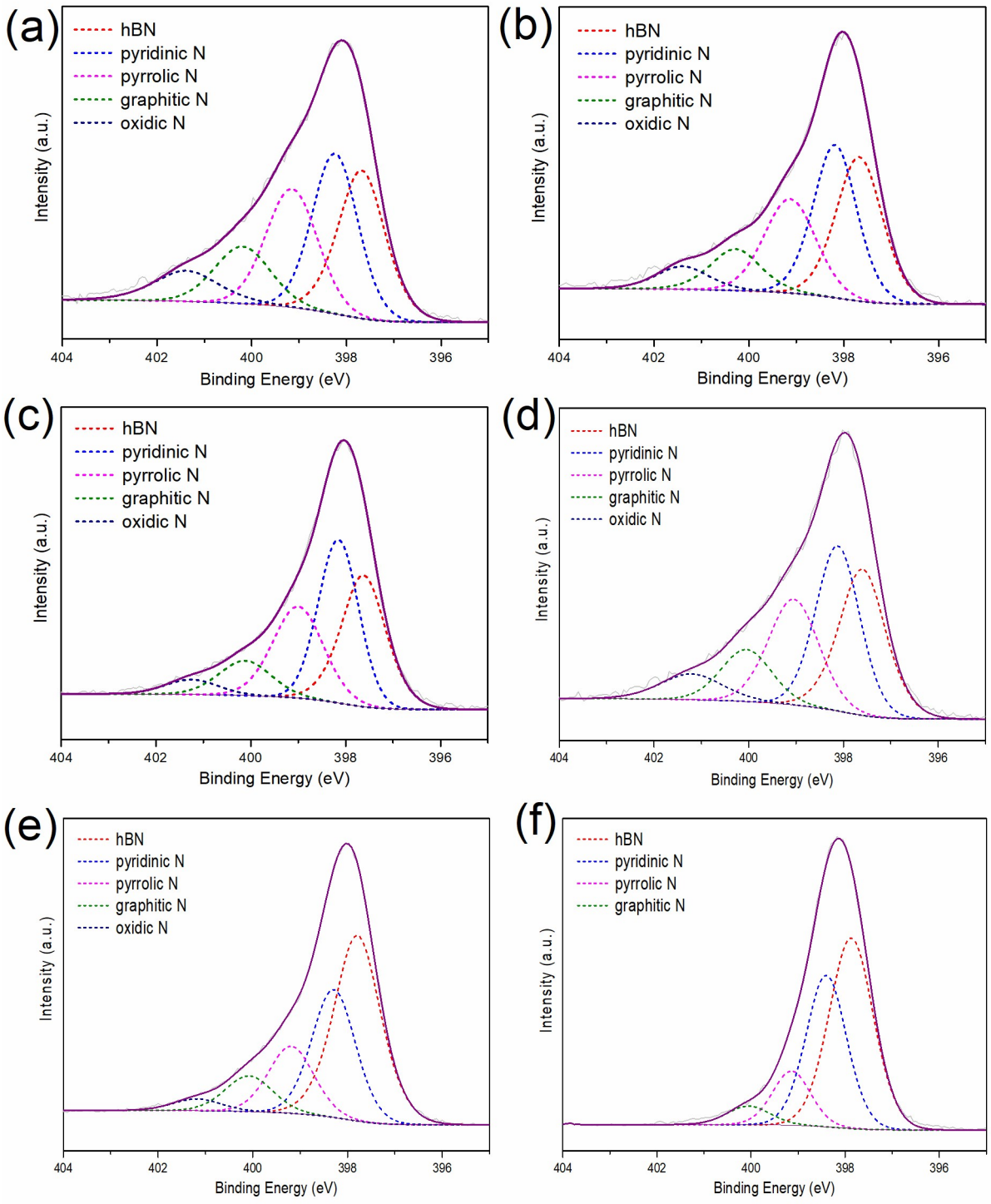

Figure S5. Deconvoluted XPS N1s peak of (a) BCN-NT/NS-1; (b) BCN-NT/NS-6; (c) BCN-NT/NS-8; (d) BCN-NT/NS-10; (e) BCN-NT/NS-8_800; (f) BCN-NT/NS-8_1000.

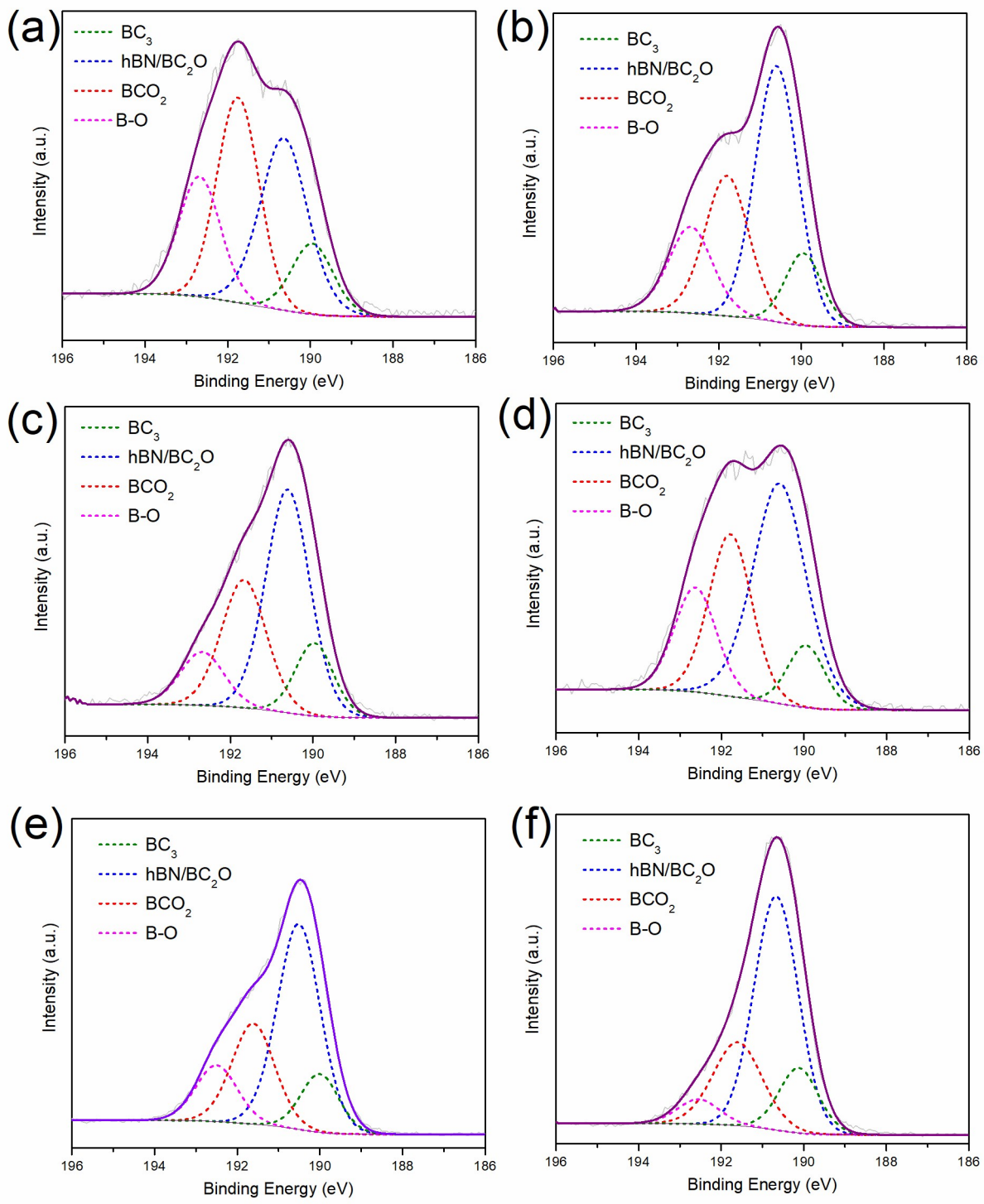

Figure S6. Deconvoluted XPS B1s peak of (a) BCN-NT/NS-1; (b) BCN-NT/NS-6; (c) BCN-NT/NS-8; (d) BCN-NT/NS-10; (e) BCN-NT/NS-8_800; (f) BCN-NT/NS-8_1000.

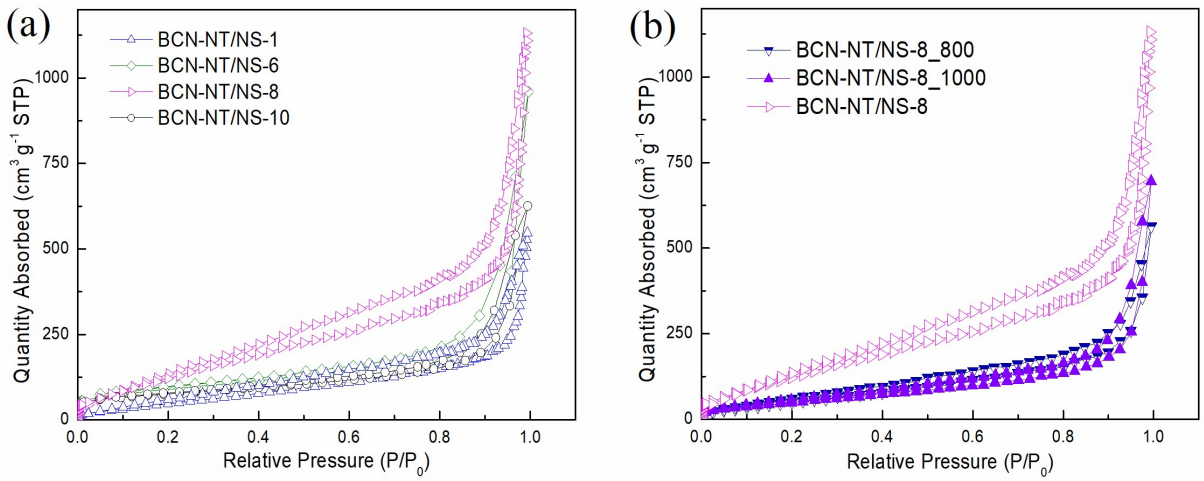

Figure S7. Nitrogen adsorption-desroption isotherms of (a) BCN-NT/NS composites prepared with different PEG precursors; (b) BCN-NT/NS composites prepared at different temperatures.

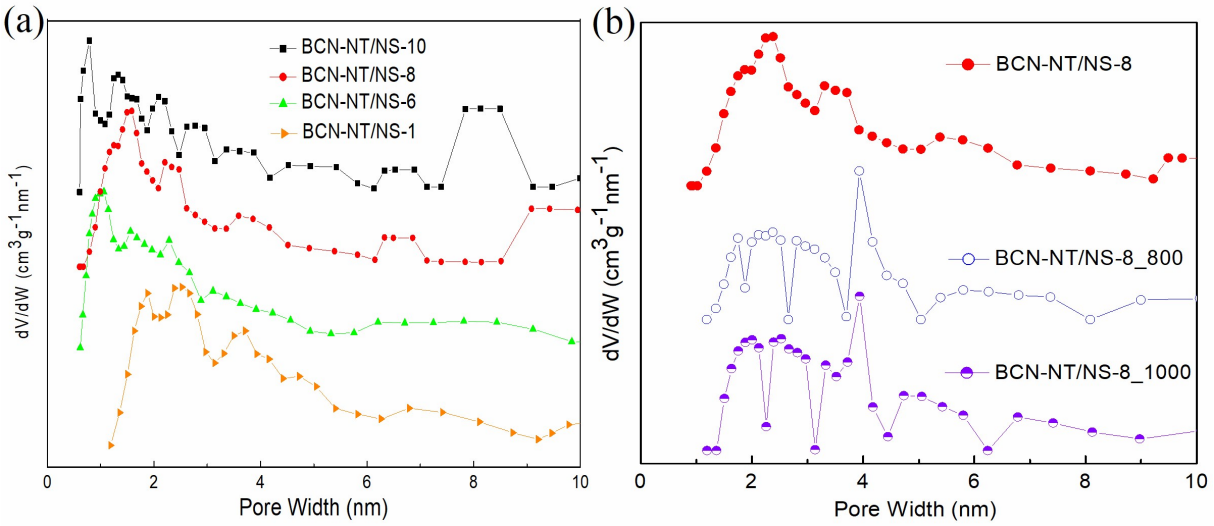

Figure S8. Pore size distribution of (a) BCN-NT/NS composites prepared with different PEG precursors; (b) BCN-NT/NS composites prepared at different temperatures.

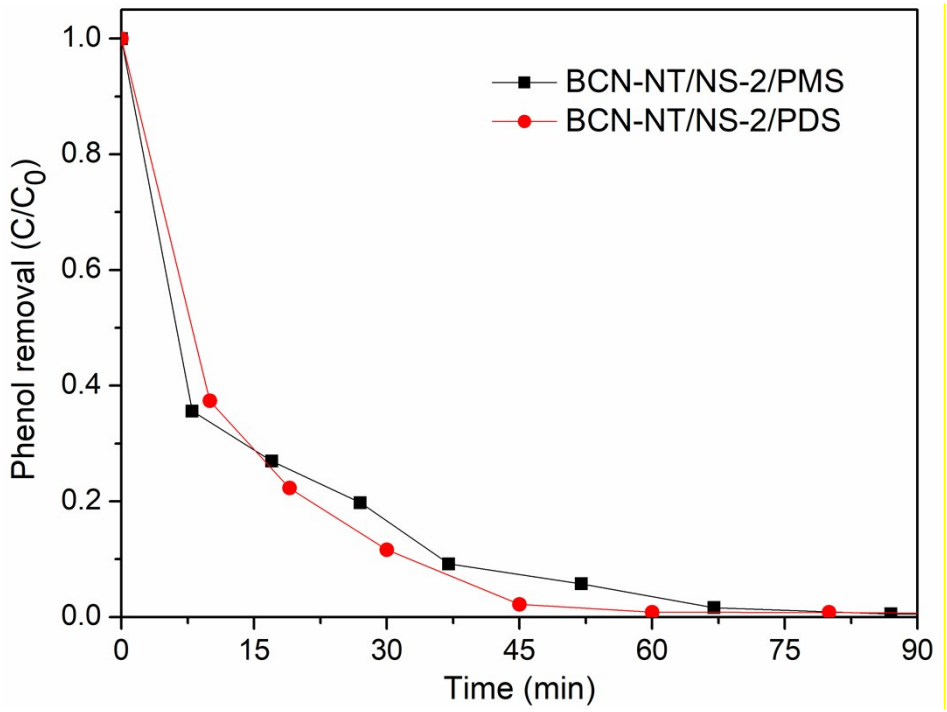

Figure S9. PDS and PMS activation for oxidative degradation of phenol by BCN-NT/NS-2. Conditions: [Catalyst] = 0.2 g/L, [Persulfate]= 2 g/L, $[Phenol]_0$ = 100 ppm.

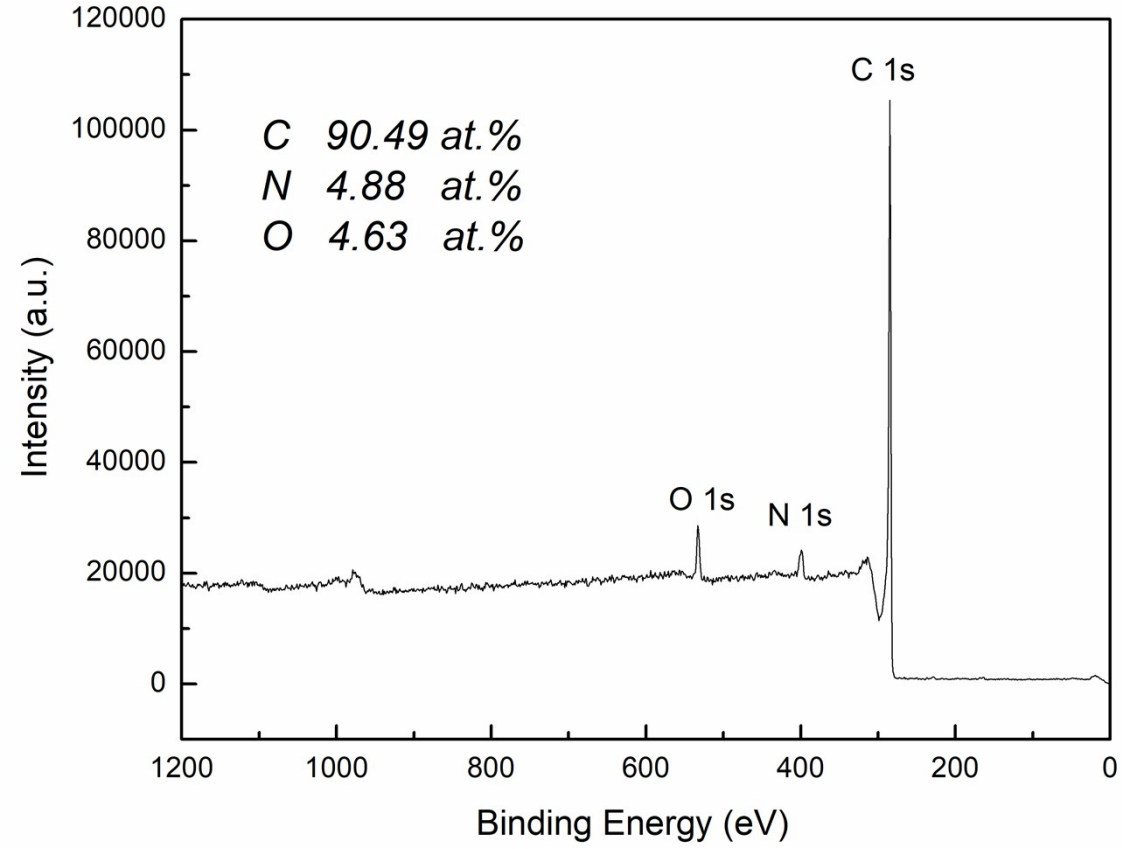

Figure S10. XPS survey spectrum of N-rGO.

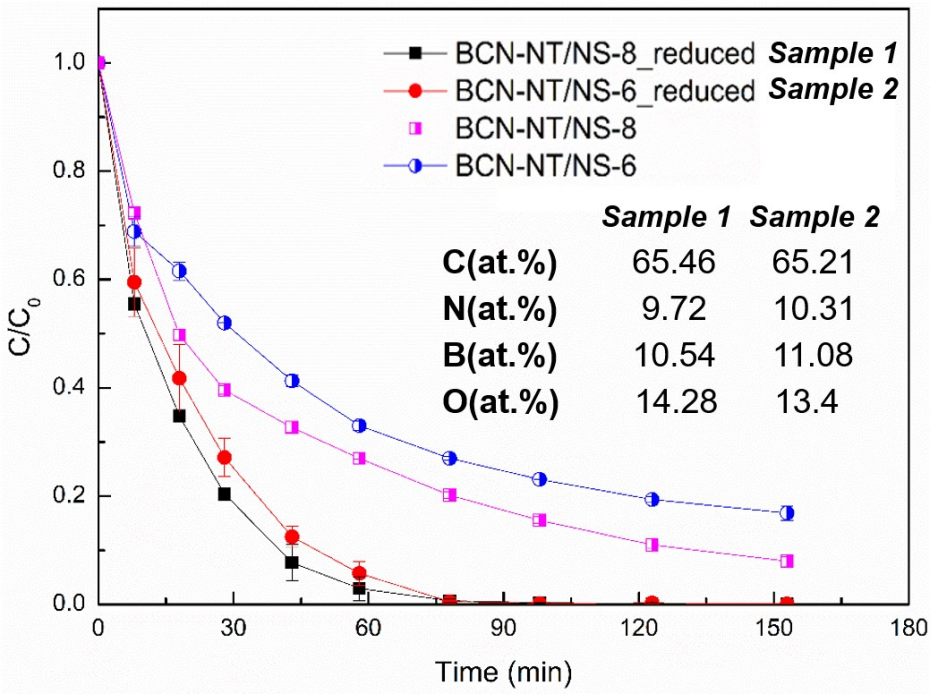

Figure S11. PDS activation for oxidative degradation of phenol by BCN-NT/NS-8, BCN-NT/NS-6 and the corresponding reduced samples. Conditions: [Catalyst] = 0.2 g/L, [PDS]= 7.4 mM, $[Phenol]_0$ = 200 ppm.

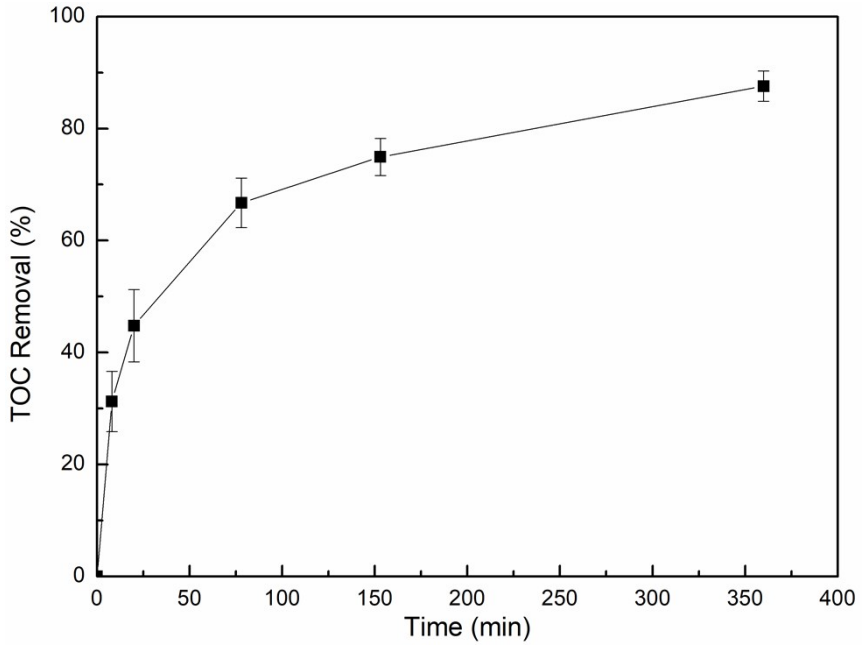

Figure S12. TOC removal during the phenol degradation process by BCN-NT/NS-8/PDS system. Conditions: $[Phenol]_0$ = 200 ppm, $[PDS]_0$ = 7.4 mM, $[Catalyst]_0$ = 0.2 g L^{-1}.

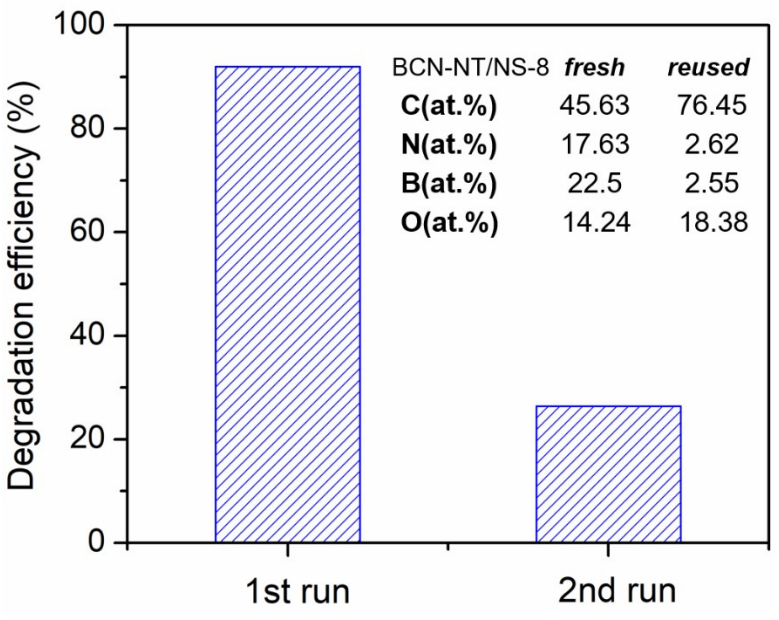

Figure S13. Cycling test of BCN-NT/NS-8/PDS system for phenol degradation and the elemental composition of reused BCN-NT/NS-8 by XPS analysis. Conditions: $[Phenol]_0$ = 200 ppm, $[PDS]_0$ = 7.4 mM, $[Catalyst]_0$ = 0.2 g L^{-1}.

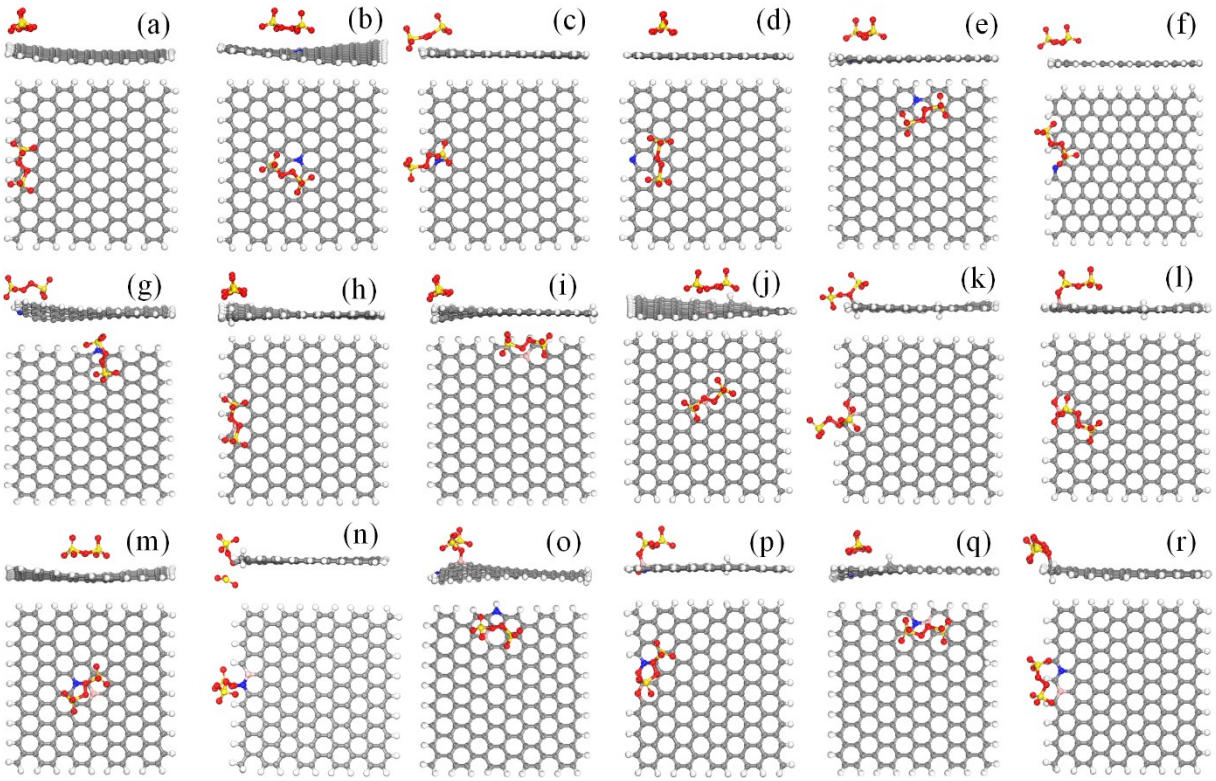

Figure S14. The most stable configuration of $S_2O_8^{2-}$ adsorbed onto (a) pristine graphene, (b) gN*i*-doped graphene, (c) gN*z*-doped graphene, (d) pdN*z*-doped graphene, (e) gN*a*-doped graphene, (f) pdN*a*-doped graphene, (g) prN-doped graphene, (h) B*z*-doped graphene, (i) B*i*-doped graphene, (j) B*a*-doped graphene, (k) BC_2O-doped graphene, (l) BCO_2-doped graphene, (m) B*i*-C-N-doped graphene, (n) B-pdN*z* pair-doped graphene, (o) B*z*-C-prN-doped graphene (p) BCO_2-gN*z*-doped graphene, (q) B-gN*a* pair-doped graphene and (r) B*z*-C-gN*z*-doped graphene.

References

1 J. P. Perdew, A. Ruzsinszky, G. I. Csonka, O. A. Vydrov, G. E. Scuseria, L. A. Constantin, X. Zhou and K. Burke, *Phys. Rev. Lett.*, 2008, **100**, 136406.

2 E. R. McNellis, J. Meyer and K. Reuter, *Phys. Rev. B*, 2009, **80**, 205414.

3 P. Jurečka, J. Černý, P. Hobza and D. R. Salahub, *J. Comput. Chem.*, 2007, **28**, 555–569.

4 A. Tkatchenko and M. Scheffler, *Phys. Rev. Lett.*, 2009, **102**, 73005.